

Continuous Variable Quantum Teleportation Network

Shaoping Shi, Yajun Wang, Long Tian, Wei Li, Yimiao Wu, Qingwei Wang, Yaohui Zheng,* and Kunchi Peng

Quantum network scales the advantages of quantum communication protocols to more than two detached users, which offers great potential to realize the quantum internet. Here, a fully connected continuous-variable (CV) quantum teleportation network architecture is presented, in which a squeezed state of light distributes each pair of entangled sideband modes to each communication link that bridges any pair of users. The quantum teleportation scheme is similar to standard two-party ones for each communication link, without sacrificing communication capability and reliability. The demonstration based on CV-entangled sideband modes opens an innovative possibility to implement many tasks of deterministic quantum information processing.

1. Introduction

The building of quantum network is an essential ingredient in the realization of the quantum internet that represents an impressive feat of science and technology, giving a chance to perform quantum information processing in city-wide metropolitan areas.^[1–4] In virtue of diverse quantum information carriers, including optical qubits,^[5,6] atomic ensembles,^[7,8] trapped atoms,^[9,10] solid state systems,^[11,12] and optical modes,^[13–15] substantial advances regarding quantum key distribution,^[16,17] quantum teleportation,^[18,19] and quantum dense coding^[20,21] have been made toward the realization of quantum network. Quantum teleportation, as the most fundamental Gaussian operation, represents a fundamental ingredient in the development of many advanced quantum technologies.^[22,23] Critical experimental capabilities have been achieved, beginning with the realization of two-party quantum information processing protocol,^[24,25] and extending to quantum network with multi-user participation.^[26]

To scale the interconnection nodes without sacrificing security or functionality relative to simple point-to-point

quantum information protocol, a multitude of diverse quantum network architectures have been experimentally achieved. The architectures can be categorized into four groups, including transparent network architecture,^[27–30] trusted relay architecture,^[31–33] multipartite (high-dimensional) entanglement based architecture,^[14,34–38] and fully connected network architecture.^[26,39,40] It should be noted that each individual architecture has both advantages that may be compatible with network construction and disadvantages that influence reliability, security, and efficiency of communication. A recent experiment

demonstrates a fully interconnected network that offers substantial advances in network performance, based on multiplexing and bipartite entanglement photons.^[26,39] Further, the amount of users was doubled in combination with beam splitters, promising an extensible performance of multiple users without resorting to the increase of wavelength channel.^[39,41] Compared with the scenario, the continuous variable (CV) physical system enjoys deterministic quantum state generation, unconditional operations, and ultrahigh detection efficiencies,^[42–44] which represent the complementary physical system with respect to the discrete-variable system. However, fully interconnected quantum network with more than two users based on CV has not been demonstrated due to challenges in implementing demultiplexing and multiplexing operations with ultra-low losses.

In this article, we report the first demonstration of a fully interconnected quantum teleportation network for a CV optical system, which is realized by applying the entangled sideband optical modes from a squeezed state of light.^[45–47] A significant advance of our demonstration is that fully connected quantum network demonstrated here is realized deterministically and verified without post selection. We distribute each pair of entangled sideband optical modes and perform quantum teleportation protocol between any pair of users; thus, the challenge of severe decoherence from the demultiplexing and multiplexing processes is overcome. Each user linked to the network has its own communication link with any other user at the same time, ensuring the exactly same quantum teleportation scheme as standard two-party ones, offering a substantial boost in terms of reliability without limiting the communication capability.

2. Experimental Setup

Here, we consider the generation of continuous variable non-classical states through an optical parametric oscillator (OPO),

S. Shi, Y. Wang, L. Tian, W. Li, Y. Wu, Q. Wang, Y. Zheng, K. Peng
State Key Laboratory of Quantum Optics and Quantum Optics Devices
Institute of Opto-Electronics
Shanxi University
Taiyuan 030006, China
E-mail: yzheng@sxu.edu.cn

Y. Wang, L. Tian, W. Li, Y. Zheng, K. Peng
Collaborative Innovation Center of Extreme Optics
Shanxi University
Taiyuan 030006, China

 The ORCID identification number(s) for the author(s) of this article can be found under <https://doi.org/10.1002/lpor.202200508>

DOI: 10.1002/lpor.202200508

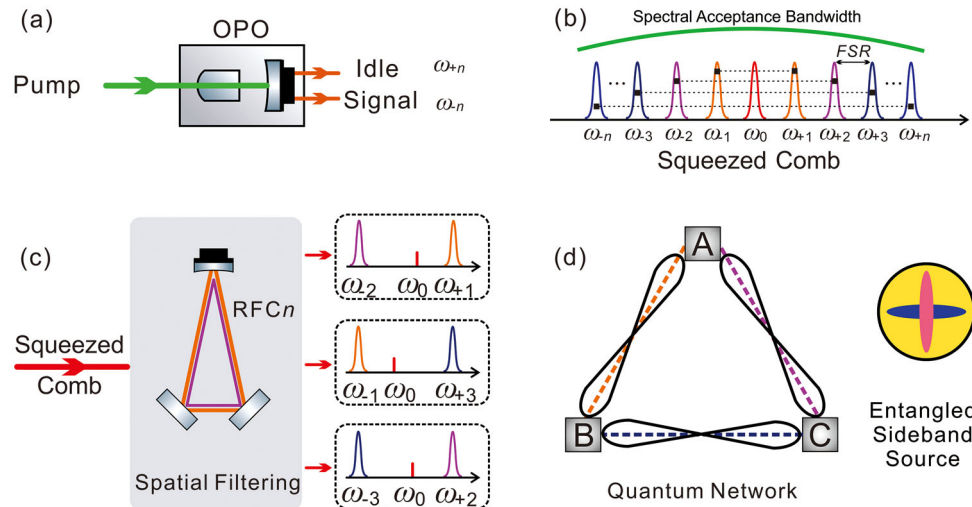


Figure 1. Schematic diagram of the CV quantum teleportation network. a) Squeezed light is generated using a sub-threshold OPO with PPKTP as its nonlinear medium. b) Sideband modes of squeezed light show the frequency-comb characteristics, and symmetrical of them exhibit entangled correlation. c) Utilizing ring filter cavity to achieve spatial separation of entangled sidebands. d) All users fully connected quantum network.

in which a pump photon at frequency $2\omega_0$ splits into a pair of lower-energy photons via second order nonlinear interaction process shown in **Figure 1**. The downconversion optical field covers a continuous spectrum within phase-matching bandwidth of the nonlinear medium. An optical cavity can serve as nonlinear interaction enhancement, but the down converted output presents a comb-type spectrum, the bandwidth of which is determined by the cavity linewidth. Each pair of symmetric downconversion fields ω_{-n} and ω_{+n} around the frequency ω_0 presents a non-classical correlation, where $\omega_{\pm n} = \omega_0 \pm n \cdot FSR$, FSR is the cavity free spectral range, and n is an integer. The demultiplexing operation is performed by employing a cascade of low-loss frequency-dependent beam splitter. After demultiplexing, each combination of two sideband modes is distributed to one of the users (Alice, Bob, and Chloe), who are linked to the network via a single physical path. Using the demultiplexing and distributing process, any two users share bipartite entangled sidebands, which makes sure each pair of users build their own private communication links without crosstalk effect. Since the OPO has free spectral range of 3.325 GHz that is far larger than the detection bandwidth, the detrimental impact that comes from the adjacent sideband modes can be completely neglected by selectively detecting the desired wavelengths with the assistance of frequency-tuning local oscillator (LO).

With the experimental setup shown in **Figure 2**, we implement a full-connected quantum communication network with three users by applying three pairs of EPR sideband modes from a squeezed field. The bright squeezed state of light is generated by a sub-threshold OPO operating at parametric deamplification, which has been detailedly demonstrated in our previous literatures.^[48,49] The higher-order sideband modes of the squeezed light have no coherent amplitude, hindering the extraction of error signal for active control in the downstream experiment.^[50,51] We construct a frequency-comb-type control beam that has the same frequency and phase with each corresponding entanglement sidebands by exploiting the waveguide

electro-optical modulator (WGM1) to convert vacuum sideband modes to bright optical modes.^[52]

The wide spectrum of the down-converted field multiplexing in single physical path is allocated to three groups of sideband modes by employing three low-loss ring filter cavities (RFCs). We accomplish the demultiplexing and multiplexing processes by designing the special RFCs that can transmit two asymmetric sidebands to reduce the loss as much as possible.^[52] Three groups of sideband modes are spatially separated and distributed to three detached users Alice (sideband modes ω_{-2} and ω_{+1}), Bob (sideband modes ω_{-1} and ω_{+3}), and Chloe (sideband modes ω_{-3} and ω_{+2}). Following the distribution scheme, Alice and Bob share the first-order entangled sideband modes, whereas Alice and Chloe (Bob and Chloe) share the second-order (third-order) ones. Therefore, each user linked to the network shares one pair of entangled sideband modes with every other user simultaneously, making sure the quantum teleportation protocols using entangled sideband modes as a resource are implemented. In order to balance the correlation noise variances at each communication link, all these error signals for the length stability of RFCs are extracted from the transmission end of each RFC. The electro-optical modulator (EOM1) serves for the stability of the length of RFCs and the relative phase between the squeezed state and control beam. We impose a modulation frequency of 35.0 MHz that is smaller than the linewidth of all three RFCs on the EOM1, ensuring that the corresponding modulation sidebands can be transmitted from resonating RFC.

The combination of WGM2 and subsequent two mode cleaners (MCs) serve as the generation of LOs, as well as the input states and auxiliary beam (Aux) for teleportation process.^[43] The frequency of the LOs and input states can be conveniently switched by manipulating the modulation frequency of WGM2, and resonant frequency of two MCs. Two function generators that drive the WGM1 and WGM2 are synchronized by a 10 MHz RF signal to ensure the stability of the downstream phase. The EOM2 is driven by a modulation frequency of 120 MHz, which

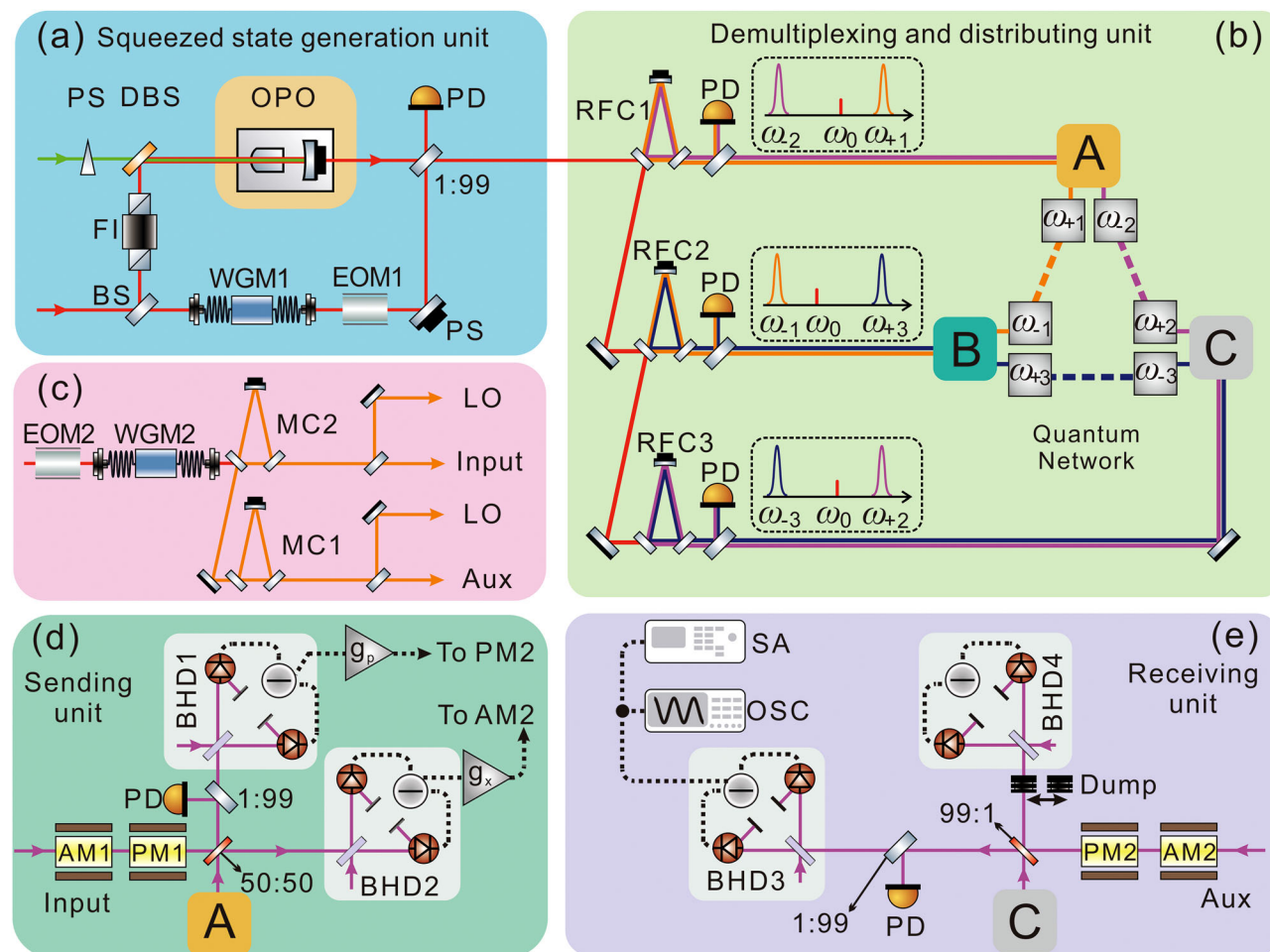


Figure 2. Schematic of experimental setup for CV quantum teleportation network. a) Generation of squeezed light and corresponding frequency-comb-type control beam. b) Demultiplexing and distributing of the sideband optical modes. c) Generation of the LOs, Input state and Aux beam. d,e) Quantum teleportation protocol from Alice to Chloe. PD, photo detector; MC, mode cleaner; EOM, electro-optical modulator; WGM, waveguide electro-optical modulator; OPO, optical parametric oscillator; BHD, balanced homodyne detector; PS, phase shifter; RFC, ring filter cavity; FI, Faraday isolator; DBS, dichroic beam splitter; LO, local oscillator; Aux, auxiliary beam; AM, amplitude modulator; PM, phase modulator; BS, beam splitter; SA, spectrum analyzer; OSC, oscilloscope.

is much larger than the linewidth of MCs (2 MHz). It can be inferred that the transmissivity of the modulation sidebands is less than 7.6×10^{-5} ; thus, the modulation interference for downstream experiment is neglected.

Each of the three users is equipped with a sending unit that extracts the amplitude and phase information of input state, and a receiving unit that reconstructs the unknown quantum state, with different configurations in mind. In virtue of the sending and receiving units, each user can teleport a quantum state to every other user linked to the network and reconstruct the teleported state from every other user in turn. For each communication link, the quantum teleportation scheme is similar to standard two-party ones^[43]; the two sideband modes that are distributed to each party are spatially separated by a frequency-dependent beam splitter, which independently serve for the other two parties. Since the two sideband modes locate at different resonances of the OPO with the large frequency intervals, the cross-talking effect can be totally avoided.

Taking the teleportation operation from Alice to Chloe as an example, the input state that has the same frequency as sideband ω_{-2} is combined with the entangled sideband modes (ω_{-2}) that is distributed to the user Alice, at a balanced beam splitter (with a relative phase of 0) to perform a joint measurement. Taking advantage of two LOs with the same frequency as sideband ω_{-2} , the amplitude and phase information are acquired by BHD1 and BHD2 and dispatched to Chloe through two classical channels with proper gains.

In Chloe's terminal, an Aux, which has the same frequency as the sideband ω_{+2} , obtains the teleported information by utilizing an amplitude modulator (AM2) and a phase modulator (PM2). The Aux carrying the acquired information is combined with entangled sideband modes (ω_{+2}) at a 99:1 beam splitter to reassemble the initial input state. The BHD3 is utilized to verify the performance of the reassembled state with the assistance of LO that has same frequency as ω_{+2} . The alternating current signal of the BHD3 is utilized to reconstruct the Wigner function with

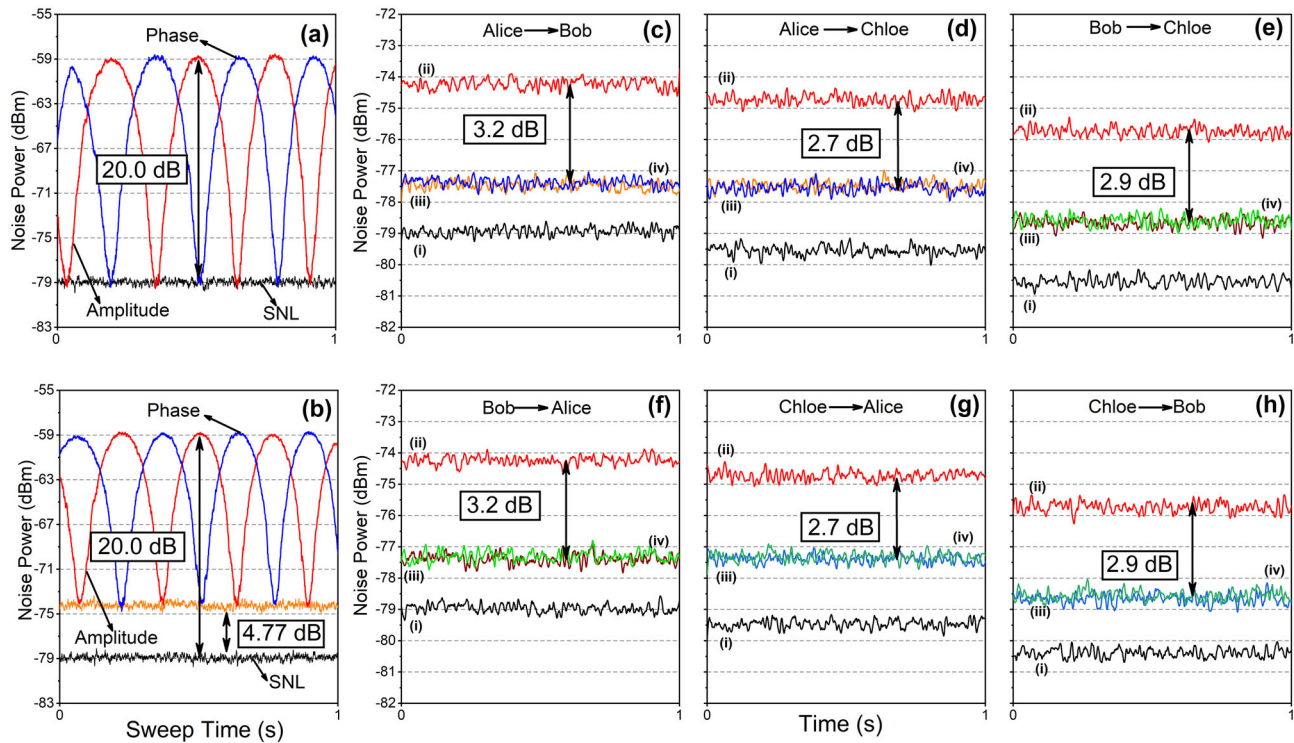


Figure 3. Gain optimization and experimental results. a) Noise power of a coherent input beam with a modulation amplitude of 20 dB. b) Noise power recorded by receiver while scanning the relative phases between “Aux” and “local oscillator of BHD3,” demonstrating that the peak amplitudes input and output amplitudes are equal, and the amplitude and phase quadratures are $\pi/2$ apart in phase. c–h) Noise powers of the teleported state measured by receiver with all users in quantum network as sending and receiving terminals. All traces are recorded via spectrum analyzer with an analysis frequency of 3.0 MHz (RBW, 100 kHz; VBW, 100 Hz). In subfigures (c)–(h), trace (i) represents the SNL, which is obtained by only injecting local oscillator into the BHDs. Trace (ii) shows the noise power of the teleported state without EPR entanglement, and it is 4.77 dB higher than the SNL as expected. Traces (iii) and (iv) are the noise power for amplitude and phase quadrature of the teleported state with the help of EPR entanglement.

an oscilloscope and to obtain the noise power of the reassembled state with a spectrum analyzer. Similarly, the teleportation operation can also be realized between any two users by conveniently switching the frequency of the LOs, input states, and Aux beams.

3. Experimental Results

Before teleportation process, the correlation noise variances of the three users are measured by utilizing the existing instruments. We obtain the total noise variance of the sending unit from the output signals of BHD 1 and BHD 2. The noise variance of the receiving unit is measured by BHD 3. Then, it is combined with the output of BHD 1 and BHD 2 to read the correlation noise. The correlation noises of amplitude sum and phase difference for Alice and Bob (Alice and Chloe and Bob and Chloe) are unbiased and equal to 6.7 dB (5.2 and 5.8 dB).

A crucial part of the teleportation protocol is the transmission of classical information from sending terminal to receiving terminal. To ensure that the signals are transmitted without distortion, the gain factors for both amplitude (g_x) and phase (g_p) quadratures should be fixed to be unity. **Figure 3a,b** shows the calibration results of the gain factors with a coherent state as input state. **Figure 3a** is the spectral density of input state with a modulation amplitude of 20 dB, while **Figure 3b** is the spectral density recorded by receiver’s detectors. We know from the results that

receiver records equal spectral density for both the amplitude-modulated and phase-modulated input, indicating that the gain factors have been properly calibrated.

Figure 3c–h represents the experimental results of all communication links of quantum teleportation network, including from Alice to Bob (c), from Alice to Chloe (d), from Bob to Chloe (e), from Bob to Alice (f), from Chloe to Alice (g), and from Chloe to Bob (h). All traces are receiver’s measured noise variances at 3 MHz with a vacuum state as the input state. With the entangled sideband modes presenting, the noise variances are shown in trace (iii) and (iv), while with the entangled sideband modes absent, the noise variances are shown in trace (ii). Since the entangled sideband modes present unbiased feature, the noise powers of amplitude and phase quadratures are approximately equal for each teleportation process. For any pair of users, the teleportation results mainly depend on the correlation noise of the entangled states as the resource state, showcasing the user-independent characteristics. The entangled sideband modes lead to a quantum noise reduction of 3.2 dB (Alice and Bob), 2.7 dB (Alice and Chloe), and 2.9 dB (Bob and Chloe), respectively. In current experiment, the fidelity of the reassembled state is calculated to be $F_{AB} = 0.82 \pm 0.02$, $F_{BC} = 0.79 \pm 0.02$, and $F_{AC} = 0.77 \pm 0.01$, respectively.^[52]

The Wigner function, a quasiprobability distribution of quadrature amplitude and phase in phase space, provides the

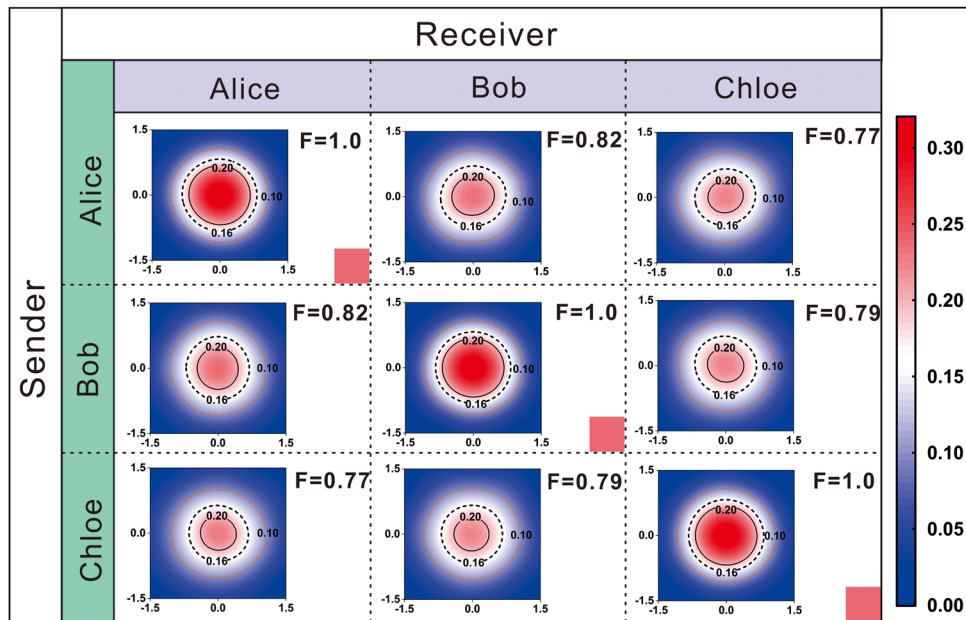


Figure 4. The counter projections of the reconstructed Wigner function in phase space of the states between all pairs of users in quantum network, via the iterative maximum-likelihood estimation. The black-circle, black-dashed-circle, and orange-dashed-dotted-circle represent the noise contours of the reconstructed Wigner function distribution at 0.2, 0.16, and 0.1, respectively. As the fidelity decreases, the contours become sparse and appear increasingly distorted from perfect circles. The photocurrent from BHD of receiving unit passes through a high-pass-filter with a cutoff frequency of 1.8 MHz and a low-pass-filter with a cutoff frequency of 4.5 MHz subsequently, and is then mixed with a demodulation sinusoidal signal at 3 MHz to extract the time-domain information from data collected by the oscilloscope with a sampling rate at 10 MS/s.

complete quantum characteristics of a quantum state, as shown in **Figure 4**. To completely characterize the performance of quantum teleportation network, the Wigner functions of reassembled states covering all sending and receiving terminals are reconstructed with the entangled sideband states by using optical homodyne tomography. Quantum tomography^[57,58] is one of universal technique which extracts the time-domain signal by the BHD, further calculate the marginal probability distribution function of the quantum state, and then obtain the quantum state density matrix and the phase space Wigner function. The three illustrations marked with red corner square in diagonal line of **Figure 4** represent the Wigner function of the input state, whereas other nondiagonal illustrations represent the Wigner function of the reassembled state between all pairs of users in quantum network. Therefore, we achieve a quantum teleportation network with three users with minimum fidelity beyond the no-cloning limit.

4. Conclusion

In conclusion, we have demonstrated a fully connected quantum teleportation network based on CV entangled sideband modes from a squeezed state of light. Since the three quantum channels are located at different resonances of the OPO that are far more than the bandwidth of the BHDs, the cross-talking effect can be totally eliminated. The topological structure effectively promotes the network reliability and flexibility, but the communication links become increasingly complex and grow quadratically as the number of users increases. On the basis of free-space filter cavity, the scheme becomes unmanageable as the num-

ber of parties increases. Fortunately, the OPO and filter cavity have been achieved based on waveguide^[59] and integrated silicon-based materials.^[60–62] In such a new filter cavity configuration, the stable control of the entire system can be achieved through passive methods such as temperature control,^[63] thereby greatly reducing the difficulty and complexity of control.

In addition, the waveguide quantum memory with an acceptance bandwidth up to 5 GHz has been demonstrated,^[64] which is compatible with our experimental protocol to perform quantum repeater. Our demonstration of CV quantum teleportation network can be also easily extended to other wavelengths that are suitable for solid state quantum memory^[65] and alkali atoms' transition line.^[66,67] Exploiting the distribution scheme of CV entangled sideband modes, a quantum network that implements many tasks of quantum information processing, without the limitation of teleportation protocol, can be realized. As the technology improves, we have enough reason to expect and believe that a fully connected continuous-variable quantum teleportation network with more parties will have a bright future.

Supporting Information

Supporting Information is available from the Wiley Online Library or from the author.

Acknowledgements

S.S., Y.W., and L.T. contributed equally to this work. This work was supported by the National Natural Science Foundation of China (NSFC)

(Grants No. 62225504, No. 62027821, No. 11874250, No. 62035015, No. 12174234 and No. 12274275); the National Key R&D Program of China (Grant No. 2020YFC2200402); the Program for Sanjin Scholar of Shanxi Province.

Conflict of Interest

The authors declare no conflict of interest.

Data Availability Statement

The data that support the findings of this study are available from the corresponding author upon reasonable request.

Keywords

quantum networks, quantum teleportation, sideband entanglement

Received: July 7, 2022

Revised: August 23, 2022

Published online:

- [1] P. V. Loock, S. L. Braunstein, *Phys. Rev. Lett.* **2000**, *84*, 3482.
- [2] S.-H. Wei, B. Jing, X.-Y. Zhang, J.-Y. Liao, C.-Z. Yuan, B.-Y. Fan, C. Lyu, D.-L. Zhou, Y. Wang, G.-W. Deng, H.-Z. Song, D. Oblak, G.-C. Guo, Q. Zhou, *Laser & Photon. Rev.* **2022**, *16*, 2100219.
- [3] Y.-A. Chen, Q. Zhang, T.-Y. Chen, W.-Q. Cai, S.-K. Liao, J. Zhang, K. Chen, J. Yin, J.-G. Ren, Z. Chen, S.-L. Han, Q. Yu, K. Liang, F. Zhou, X. Yuan, M.-S. Zhao, T.-Y. Wang, X. Jiang, L. Zhang, W.-Y. Liu, Y. Li, Q. Shen, Y. Cao, C.-Y. Lu, R. Shu, J.-Y. Wang, L. Li, N.-L. Liu, F. Xu, X.-B. Wang, et al., *Nature* **2021**, *589*, 214.
- [4] H. J. Kimble, *Nature* **2008**, *453*, 1023.
- [5] D. Gottesman, I. L. Chuang, *Nature* **1999**, *402*, 390.
- [6] Y. Zhong, H.-S. Chang, A. Bienfait, É. Dumur, M.-H. Chou, C. R. Conner, J. Grebel, R. G. Povey, H. Yan, D. I. Schuster, A. N. Cleland, *Nature* **2021**, *590*, 571.
- [7] L.-M. Duan, M. D. Lukin, J. I. Cirac, P. Zoller, *Nature* **2001**, *414*, 413.
- [8] Z. H. Yan, L. Wu, X. J. Jia, Y. H. Liu, R. J. Deng, S. J. Li, H. Wang, C. D. Xie, K. C. Peng, *Nat. Commun.* **2017**, *8*, 718.
- [9] J. Beugnon, M. P. A. Jones, J. Dingjan, B. Darquié, G. Messin, A. Browaeys, P. Grangier, *Nature* **2006**, *440*, 779.
- [10] J. Volz, M. Weber, D. Schlenk, W. Rosenfeld, J. Vrana, K. Saucke, C. Kurtsiefer, H. Weinfurter, *Phys. Rev. Lett.* **2006**, *96*, 030404.
- [11] E. Togan, Y. Chu, A. S. Trifonov, L. Jiang, J. Maze, L. Childress, M. V. G. Dutt, A. S. Sørensen, P. R. Hemmer, A. S. Zibrov, M. D. Lukin, *Nature* **2010**, *466*, 730.
- [12] L. Steffen, Y. Salathe, M. Oppliger, P. Kurpiers, M. Baur, C. Lang, C. Eichler, G. Puebla-Hellmann, A. Fedorov, A. Wallraff, *Nature* **2013**, *500*, 319.
- [13] X. Li, Q. Pan, J. Jing, J. Zhang, C. Xie, K. Peng, *Phys. Rev. Lett.* **2002**, *88*, 047904.
- [14] F. A. S. Barbosa, A. S. Coelho, L. F. Muñoz-Martínez, L. Ortiz-Gutiérrez, A. S. Villar, P. Nussenzeig, M. Martinelli, *Phys. Rev. Lett.* **2018**, *121*, 073601.
- [15] M. Wang, Y. Xiang, H. Kang, D. Han, Y. Liu, Q. He, Q. Gong, X. Su, K. Peng, *Phys. Rev. Lett.* **2020**, *125*, 260506.
- [16] F. Grosshans, G. Van Assche, J. Wenger, R. Brouri, N. J. Cerf, P. Grangier, *Nature* **2003**, *421*, 238.
- [17] F.-X. Wang, W. Wang, R. Niu, X. Wang, C.-L. Zou, C.-H. Dong, B. E. Little, S. T. Chu, H. Liu, P. Hao, S. Liu, S. Wang, Z.-Q. Yin, D.-Y. He, W. Zhang, W. Zhao, Z.-F. Han, G.-C. Guo, W. Chen, *Laser & Photon. Rev.* **2020**, *14*, 1900190.
- [18] C. H. Bennett, G. Brassard, C. Crépeau, *Phys. Rev. Lett.* **1993**, *70*, 1895.
- [19] D. Guzman-Silva, R. Brünig, F. Zimmermann, C. Vetter, M. Gräfe, M. Heinrich, S. Nolte, M. Duparré, A. Aiello, M. Ornigotti, A. Szameit, *Laser & Photon. Rev.* **2016**, *10*, 317.
- [20] K. Mattle, H. Weinfurter, P. G. Kwiat, A. Zeilinger, *Phys. Rev. Lett.* **1996**, *76*, 4656.
- [21] S. L. Braunstein, P. V. Loock, *Rev. Mod. Phys.* **2005**, *77*, 513.
- [22] M. Riebe, H. Häffner, C. F. Roos, W. Hänsel, J. Benhelm, G. P. T. Lancaster, T. W. Körber, C. Becher, F. Schmidt-Kaler, D. F. V. James, R. Blatt, *Nature* **2004**, *429*, 734.
- [23] S. Takeda, T. Mizuta, M. Fuwa, P. V. Loock, A. Furusawa, *Nature* **2013**, *500*, 315.
- [24] N. Takei, H. Yonezawa, T. Aoki, A. Furusawa, *Phys. Rev. Lett.* **2005**, *94*, 220502.
- [25] S. Pirandola, J. Eisert, C. Weedbrook, A. Furusawa, S. L. Braunstein, *Nat. Photonics* **2015**, *9*, 641.
- [26] S. Wengerowsky, S. K. Joshi, F. Steinlechner, H. Hübel, R. Ursin, *Nature* **2018**, *564*, 225.
- [27] H. Yonezawa, T. Aoki, A. Furusawa, *Nature* **2004**, *431*, 430.
- [28] T.-Y. Chen, J. Wang, H. Liang, W.-Y. Liu, Y. Liu, X. Jiang, Y. Wang, X. Wan, W.-Q. Cai, L. Ju, L.-K. Chen, L.-J. Wang, Y. Gao, K. Chen, C.-Z. Peng, Z.-B. Chen, J.-W. Pan, *Opt. Express* **2010**, *18*, 27217.
- [29] M. Sasaki, M. Fujiwara, H. Ishizuka, W. Klaus, K. Wakui, M. Takeoka, S. Miki, T. Yamashita, Z. Wang, A. Tanaka, K. Yoshino, Y. Nambu, S. Takahashi, A. Tajima, A. Tomita, T. Domeki, T. Hasegawa, Y. Sakai, H. Kobayashi, T. Asai, K. Shimizu, T. Tokura, T. Tsurumaru, M. Matsui, T. Honjo, K. Tamaki, H. Takesue, Y. Tokura, J. F. Dynes, A. R. Dixon, et al., *Opt. Express* **2011**, *19*, 10387.
- [30] S. Wang, W. Chen, Z.-Q. Yin, H.-W. Li, D.-Y. He, Y.-H. Li, Z. Zhou, X.-T. Song, F.-Y. Li, D. Wang, H. Chen, Y.-G. Han, J.-Z. Huang, J.-F. Guo, P.-L. Hao, M. Li, C.-M. Zhang, D. Liu, W.-Y. Liang, C.-H. Miao, P. Wu, G.-C. Guo, Z.-F. Han, *Opt. Express* **2014**, *22*, 21739.
- [31] J. Roslund, R. M. de Araújo, S. Jiang, C. Fabre, N. Treps, *Nat. Photonics* **2014**, *8*, 109.
- [32] S.-K. Liao, W.-Q. Cai, J. Handsteiner, B. Liu, J. Yin, L. Zhang, D. Rauch, M. Fink, J.-G. Ren, W.-Y. Liu, Y. Li, Q. Shen, Y. Cao, F.-Z. Li, J.-F. Wang, Y.-M. Huang, L. Deng, T. Xi, L. Ma, T. Hu, L. Li, N.-L. Liu, F. Koidl, P. Wang, Y.-A. Chen, X.-B. Wang, M. Steindorfer, G. Kirchner, C.-Y. Lu, R. Shu, et al., *Phys. Rev. Lett.* **2018**, *120*, 030501.
- [33] H.-Y. Liu, X.-H. Tian, C. Gu, P. Fan, X. Ni, R. Yang, J.-N. Zhang, M. Hu, J. Cao, X. Guo, X. Hu, G. Zhao, Y.-Q. Lu, Y.-X. Gong, Z. Zhu, S.-N. Xie, *Phys. Rev. Lett.* **2021**, *126*, 020503.
- [34] M. V. Larsen, X. S. Guo, C. R. Breum, J. S. Neergaard-Nielsen, U. L. Andersen, *Science* **2019**, *366*, 369.
- [35] W. Asavanant, Y. Shiozawa, S. Yokoyama, B. Charoensombutamon, H. Emura, R. N. Alexander, S. Takeda, J. Yoshikawa, N. C. Menicucci, H. Yonezawa, A. Furusawa, *Science* **2019**, *366*, 373.
- [36] W. Zhang, K. Zhang, J. Jing, *Phys. Rev. Lett.* **2020**, *125*, 140501.
- [37] X. Wang, J. Fu, S. Liu, Y. Wei, J. Jing, *Optica* **2022**, *9*, 663.
- [38] X.-M. Hu, C. Zhang, B.-H. Liu, Y. Cai, X.-J. Ye, Y. Guo, W.-B. Xing, C.-X. Huang, Y.-F. Huang, C.-F. Li, G.-C. Guo, *Phys. Rev. Lett.* **2020**, *125*, 230501.
- [39] S. K. Joshi, D. Aktas, S. Wengerowsky, M. Lončarić, S. P. Neumann, B. Liu, T. Scheidl, G. C. Lorenzo, Z. Samec, L. Kling, A. Qiu, M. Razavi, M. Stipčević, J. G. Rarity, R. Ursin, *Sci. Adv.* **2020**, *6*, eaba0959.
- [40] Y. Li, Y. Huang, T. Xiang, Y. Nie, M. Sang, L. Yuan, X. Chen, *Phys. Rev. Lett.* **2019**, *123*, 250505.
- [41] S. Armstrong, M. Wang, R. Y. Teh, Q. Gong, Q. He, J. Janousek, H.-A. Bachor, M. D. Reid, P. K. Lam, *Nat. Phys.* **2015**, *11*, 167.
- [42] S. L. Braunstein, H. J. Kimble, *Phys. Rev. Lett.* **1998**, *80*, 869.

- [43] A. Furusawa, J. L. Sørensen, S. L. Braunstein, C. A. Fuchs, H. J. Kimble, E. S. Polzik, *Science* **1998**, *282*, 706.
- [44] Q. Wang, Y. Tian, W. Li, L. Tian, Y. Wang, Y. Zheng, *Phys. Rev. A* **2021**, *103*, 062421.
- [45] J. Zhang, *Phys. Rev. A* **2003**, *67*, 054302.
- [46] B. Hage, A. Samblowski, R. Schnabel, *Phys. Rev. A* **2010**, *81*, 062301.
- [47] M. Heurs, J. G. Webb, A. E. Dunlop, C. C. Harb, T. C. Ralph, E. H. Huntington, *Phys. Rev. A* **2010**, *81*, 032325.
- [48] W. H. Yang, S. P. Shi, Y. J. Wang, W. G. Ma, Y. H. Zheng, K. C. Peng, *Opt. Lett.* **2017**, *42*, 4553.
- [49] S. P. Shi, Y. J. Wang, W. H. Yang, Y. H. Zheng, K. C. Peng, *Opt. Lett.* **2018**, *43*, 5411.
- [50] C. Schori, J. L. Sørensen, E. S. Polzik, *Phys. Rev. A* **2002**, *66*, 033802.
- [51] R. J., Senior, G. N. Milford, J. Janousek, A. E. Dunlop, K. Wagner, H. A. Bachor, T. C. Ralph, E. H. Huntington, C. C. Harb, *Opt. Express* **2007**, *15*, 5310.
- [52] See Supporting Information at [URL will be inserted by publisher], which includes refs. [53–56], for the design of asymmetric ring filter cavity, the control scheme, the correlation noise variance of entangled sideband modes, and the fidelity calculation of quantum teleportation.
- [53] S. P. Shi, L. Tian, Y. J. Wang, Y. H. Zheng, C. D. Xie, K. C. Peng, *Phys. Rev. Lett.* **2020**, *125*, 070502.
- [54] T. C. Zhang, K. W. Goh, C. W. Chou, P. Lodahl, H. J. Kimble, *Phys. Rev. A* **2003**, *67*, 033802.
- [55] L. M. Duan, G. Giedke, J. I. Cirac, P. Zoller, *Phys. Rev. Lett.* **2000**, *84*, 2722.
- [56] C. Weedbrook, S. Pirandola, R. García-Patrón, N. J. Cerf, T. C. Ralph, J. H. Shapiro, S. Lloyd, *Rev. Mod. Phys.* **2012**, *84*, 621.
- [57] K. Vogel, H. Risken, *Phys. Rev. A* **1989**, *40*, 2847.
- [58] S. Schiller, G. Breitenbach, S. F. Pereira, T. Müller, J. Mlynek, *Phys. Rev. Lett.* **1996**, *77*, 2933.
- [59] M. Stefszky, R. Ricken, C. Eigner, V. Quiring, H. Herrmann, C. Silberhorn, *Phys. Rev. Applied* **2017**, *7*, 044026.
- [60] A. Dutt, S. Miller, K. Luke, J. Cardenas, A. L. Gaeta, P. Nussenzveig, M. Lipson, *Opt. Lett.* **2016**, *41*, 223.
- [61] J. S. Levy, A. Gondarenko, M. A. Foster, A. C. Turner-Foster, A. L. Gaeta, M. Lipson, *Nat. Photonics* **2010**, *4*, 37.
- [62] G. Masada, K. Miyata, A. Politi, T. Hashimoto, J. L. O'Brien, A. Furusawa, *Nat. Photonics* **2015**, *9*, 316.
- [63] F. Kaiser, B. Fedrici, A. Zavatta, V. D'Auria, S. Tanzilli, *Optica* **2016**, *3*, 362.
- [64] E. Saglamyurek, N. Sinclair, J. Jin, J. A. Slater, D. Oblak, F. Bussi eres, M. George, R. Ricken, W. Sohler, W. Tittel, *Nature* **2011**, *469*, 512.
- [65] X. Liu, J. Hu, Z.-F. Li, X. Li, P.-Y. Li, P.-J. Liang, Z.-Q. Zhou, C.-F. Li, G.-C. Guo, *Nature* **2021**, *594*, 41.
- [66] Y. Takeno, M. Yukawa, H. Yonezawa, A. Furusawa, *Opt. Express* **2007**, *15*, 4321.
- [67] L. Ma, X. Lei, J. Yan, R. Li, T. Chai, Z. Yan, X. Jia, C. Xie, K. Peng, *Nat. Commun.* **2022**, *13*, 2368.